Desert aerosol transport in the Mediterranean region as inferred from the TOMS aerosol index

P. L. Israelevich, Z. Levin, J. H. Joseph, and E. Ganor

Department of Geophysics and Planetary Sciences, The Raymond and Beverly Sackler Faculty of Exact Sciences, Tel Aviv University, Ramat Aviv, Israel

Received 17 December 2001; revised 10 April 2002; accepted 12 April 2002; published 8 November 2002.

[1] We proposed to identify the sources of desert dust aerosols with local maxima of the TOMS aerosol index distribution averaged for the long period. Being simpler than the approach based on a dusty days occurrence, our method gives the same results. It was first shown that in spring-summer, the flux of dust from the sources located at latitude ~16°N and longitude ~16°E and around latitude ~19°N and longitude ~6°W exceed the sinks due to settling and transport. As a result the atmosphere over North Africa is almost permanently loaded with a significant amount of mineral desert dust in spring and in summer. It is also shown that the Chad basin source located around latitude 16°N and longitude 16°E is relatively more stable with a maximum activity around April. The region around latitude 19°N and longitude 6°W appears as a more variable source with maximum in July. Low pressure systems, called Sharav cyclones, mobilize the already suspended mineral dust and transport it eastward and northward along the Mediterranean basin. A new method for description of dust plumes propagation was applied to the study of dust events in the Mediterranean Sea and enabled us to follow their dynamics. Identifiable dust plumes appear first in the western sector of the sea and then move eastward with a speed of about 7 to 8 degrees per day. In spring, this motion continues at least up to the eastern coast of the Mediterranean. In summer the dustplume is prevented from penetrating further east of about 15°E. *INDEX TERMS:* 0305 Atmospheric Composition and Structure: Aerosols and particles (0345, 4801); 0322 Atmospheric Composition and Structure: Constituent sources and sinks; 4801 Oceanography: Biological and Chemical: Aerosols (0305); *KEYWORDS:* Aerosols, desert dust, dust storms, dust sources, Mediterranean

Citation: Israelevich, P. L., Z. Levin, J. H. Joseph, and E. Ganor, Desert aerosol transport in the Mediterranean region as inferred from the TOMS aerosol index, *J. Geophys. Res.*, *107*(D21), 4572, doi:10.1029/2001JD002011, 2002.

1. Introduction

[2] The role of aerosol particles in atmospheric processes is extremely important in climate research, rain formation, weather forecasting, bio-geochemical cycling as well as remote sensing of the reflectance and texture of ground and other surfaces. The aerosol forcing affects the atmosphere in two ways: (1) direct effect - in which aerosols reflect and absorb solar radiation; (2) indirect effect - when aerosols affect clouds by (a) increasing drop concentration and optical depth and (b) by reducing drop size making the clouds more stable with lower potential to produce rain. The last effect extends the lifetime of the clouds and modifies ground wetness. For this reason, systematic studies are undertaken now in order to retrieve global as well as regional distributions of aerosols. However, well known difficulties in obtaining dust particles characteristics via remote sensing methods [*Kaufman et al.*, 1997, 1998] demand also correlated (ground based, airborne, and space) observations in dedicated campaigns in specific regions (e.g., ACE 1, 2, TarFox, Scar A/B/C, Safari 2000, ACE-Asia and MEIDEX [see http://www.tau.ac.il/geophyiscs/MEIDEX/home.htm]). Such comprehensive studies and specific campaigns, along with the information on the events, will improve the methods of retrieval of aerosol parameters, and enable mutual calibration and validation of data sets. In this context, the immediate sea surface environment of the main global source of desert aerosol - the North African Desert is a convenient focus for investigation of desert dust properties and its influence on the climate in the region.

[3] Numerous works on the Mediterranean dust [e.g., *Manes and Joseph*, 1971; *Joseph et al.*, 1973; *Joseph and Wolfson*, 1975; *Joseph*, 1984; I. Koren et al., On the size and shape of dust aerosol in the Middle East, submitted to *Journal of Geophysical Research*, 2002; *Levin and Lindberg*, 1979; *Levin et al.*, 1980; *Bergametti et al.*, 1989; *Dayan et al.*, 1991; *Alpert and Ganor*, 1993, 2001; *Molinaroli et al.*, 1993; *Kubilay and Saydam*, 1995; *Loye-Pilot and Martin*, 1996; *Marticorena and Bergametti*, 1996; *Moulin et al.*, 1997, 1998; *Prospero et al.*, 2002] enabled to outline the following pattern of the desert dust transport above the Mediterranean sea. The main sources for the dust

0148-0227/02/2001JD002011$09.00

in the Mediterranean region are specific regions of the Sahara desert. *Prospero et al.* [2002] determined sources of the Saharan dust using TOMS aerosol index. The dust is transported from these sources over land and sea to regions like Europe, the Middle East and across the Atlantic to areas as far away as Mexico City. This transport occurs in spectacular storm-like events, when clouds of the desert aerosol particles take the shape of giant plumes that can span the North-South extent of the Mediterranean or cover large regions west of Africa and extend more than one thousand kilometers from the source. The enormous dust plumes, emanating from the west coast of Africa from February to September are generated by the action of low latitude easterly waves [e.g., *Karyampudi et al.*, 1999]. The main axis of transport migrates northward from about 10°N in February to 25°N in September. The total optical depth in the visible solar spectrum may reach as high as 6. Many of the plumes have a SW-NE major axis orientation, with large variability in direction. The orientation of these plumes does not correspond directly to the average atmospheric circulation that has predominant wind directions from E and NE in low latitudes to W and NW in the subtropics. The observed dust events are associated with the northward components of winds produced by synoptic depressions.

[4] Using daily satellite observations in the visible light, *Moulin et al.* [1998] identified three major situations responsible for Saharan dust transport over the Mediterranean sea in accordance with the main zones of cyclogenesis in the Mediterranean [*Alpert et al.*, 1990]. In the spring, these are Sharav cyclones [*Alpert and Ziv*, 1989] which move eastward along the North African coast and bring the dust to the eastern Mediterranean. In summer, high pressure over Libya [*Bergametti et al.*, 1989] prevents further eastward propagation of these cyclones, and the associated dust transport occurs in the central Mediterranean. At the end of the summer, low pressures near the Balearic Islands result in dust transport mainly to the western Mediterranean. The best estimate for the maximal number of dust events in a two weeks period is 3 [see *Moulin et al.*, 1998, *Ganor*, 1994, *Ganor and Foner*, 1996]. Several studies have shown the importance of these aerosols to the global and regional energy balance [*Joseph*, 1984, *Tegen et al.*, 1996, *Sokolik and Toon*, 1999], to weather forecasting [*Alpert et al.*, 1998] and to rain formation [*Levin et al.*, 1996]. These, however, represent results from limited data and are based on localized statistics. In order to study Mediterranean weather and climate it is important to obtain higher spatial-temporal resolution of the dust transport dynamics and of the aerosol type as well as their spatial and temporal correlation. In this paper we present results of a study of the desert transport to the Mediterranean basin using TOMS aerosol index.

2. UV Detection of the Desert Aerosol

[5] TOMS aerosol detection technique utilizes the spectral contrast of two ultraviolet channels, (*A* and *B*) [*Herman et al.*, 1997]. The central wavelengths of channels used for determination of the aerosol index were different for different modifications of TOMS instrument. NIMBUS-7 aerosol index was calculated for 340 nm (channel *A*) and 380 nm (channel *B*). Aerosol index from Earth Probe used 331 nm (*A*) and 360 nm (*B*) wave lengths. Since the aerosol scattering weakly depends on wavelength, its presence reduces the spectral contrast as compared to that expected for Raleigh atmosphere. Therefore, the ratio of intensities I_A/I_B can be used for detection of the presence of Mie scatterers. TOMS aerosol index incorporates also the change in backscattered radiance in channel *B*. For the fixed radiance corresponding to channel *B*, the spectral contrast is largest for non-absorbing aerosols and decreases with increasing absorption. Therefore, the aerosol index is defined as

$$AI = -100\{\log[(I_A/I_B)_{mes}] - \log[(I_A/I_B)_{mod}]\}$$

(where the indices mes and mod refer to the measured and modeled for pure Raleigh scattering, respectively) is positive for absorbing aerosols (e.g., dust and smoke particles) and negative for non-absorbing aerosols (e.g., sulfates) [*Herman et al.*, 1997; *Torres et al.*, 1998]. Moreover, for clouds, $AI \approx 0$ [*Herman et al.*, 1997], and therefore the main effect of the sub pixel clouds on the aerosol index is the partial screening of the aerosol. The TOMS radiances at the near-UV channels have been used in an inversion algorithm to derive aerosol optical depth and single scattering albedo [*Torres et al.*, 2002].

[6] The aerosol index is proportional to the single-scattering co-albedo and to the absorption optical depth (i.e., to the amount of the aerosol present in the column along the line of sight). However, it also exhibits strong dependence on the height distribution of the aerosols. In particular, this dependence significantly decreases the aerosol index sensitivity to the aerosol presence at altitudes below 1 km. In spite of that, the TOMS aerosol index measurements are linearly proportional to the aerosol optical thickness derived independently from ground-based Sun-photometer instruments over regions of biomass burning and regions covered by African dust [*Hsu et al.*, 1999]. Therefore the aerosol index is an effective measure of the dust loading in the atmosphere, and it has been successfully used to determine the dynamics of global distributions of the absorbing aerosols by *Herman et al.* [1997] and their sources *Prospero et al.* [2002].

[7] We are interested in mineral dust dynamics over the Mediterranean. Therefore, we use in this study only positive values of AI above the North Africa and Mediterranean sea provided by the TOMS instrument aboard the Earth Probe satellite (ftp://toms.gsfc.nasa.gov). The data are put into grid sizes of 1° latitude by 1.25° longitude.

3. Sources of Desert Dust for the Mediterranean

[8] Global distribution of sources of mineral dust (in particular, sources in Northern Africa) has been obtained recently by *Prospero et al.* [2002] from TOMS aerosol index provided by NIMBUS-7 measurements. They used frequency of dust events occurrence statistics, and identified regions with high dust occurrence as mineral dust sources. In order to reduce statistical "noise" introduced by low values of the aerosol index, *Prospero et al.* [2002] used a threshold filter that eliminated daily aerosol index data below a specified value.The threshold value was 1.0 for Northern Africa sources.

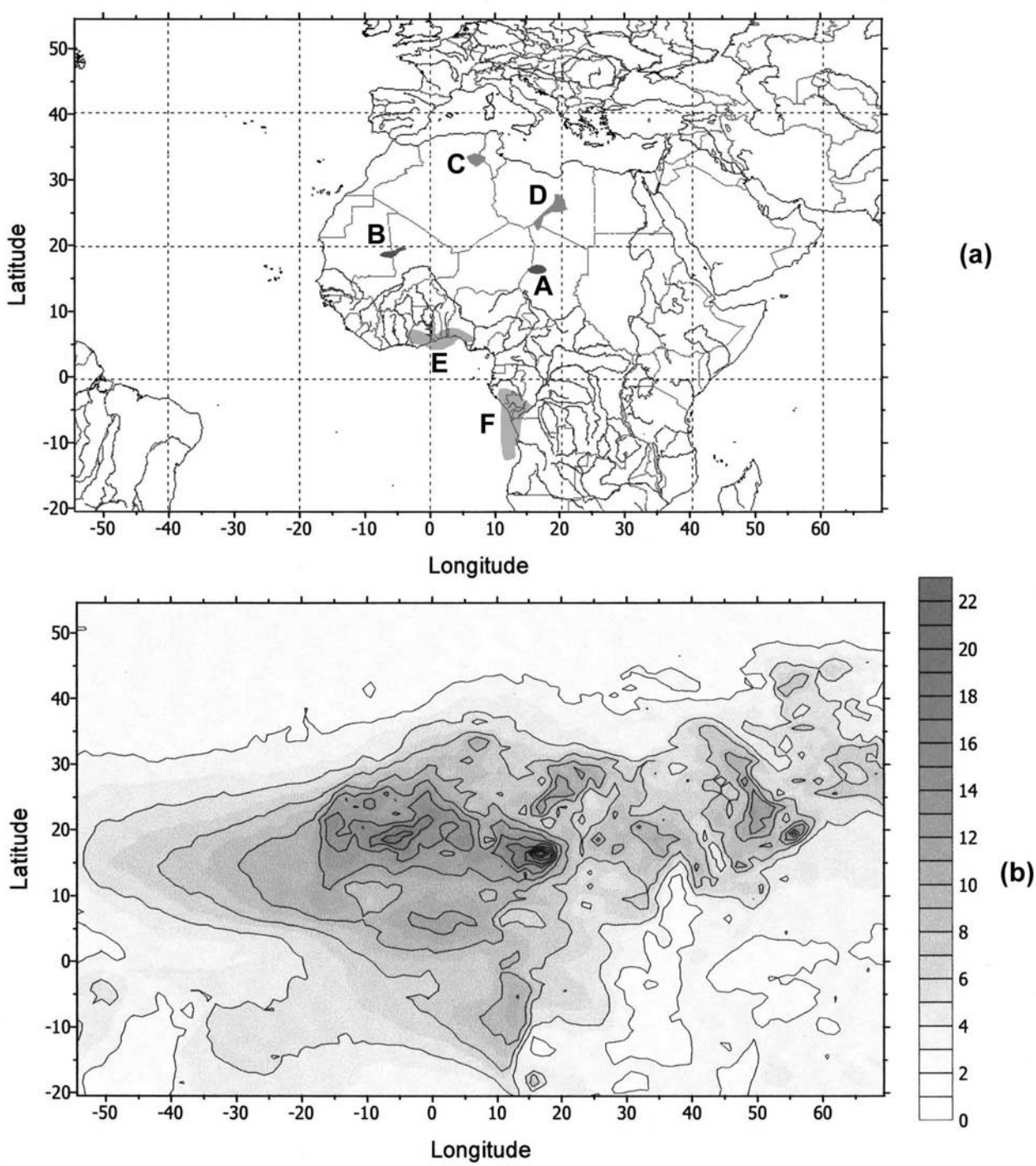

Figure 1. (a) The map of the region of interest. The shadowed areas show the main sources of UV-absorbing aerosol. (b) Distribution of the average values of the positive aerosol index above the region of interest for the period from August 1996 to April 2000. (c) Distribution of maximum values of the aerosol index observed during the period from August 1996 to April 2000. (d) Main transport ways for the desert dust.

[9] Here we perform the detection of Saharan dust sources using a different approach in handling aerosol index data which uses averaging of the aerosol index distribution over long period of time. We consider the aerosol distribution according to TOMS aerosol index in the region within latitudes range between 20.5°S to 54.5°N and longitude range from −54°W to 70°E during the period from August, 1996 to April, 2000. This region includes the Mediterranean basin and Northern Africa along with neighboring regions (Figure 1a). Figure 1b shows the 2D distribution of the average value of positive AI for each pixel for the whole period.

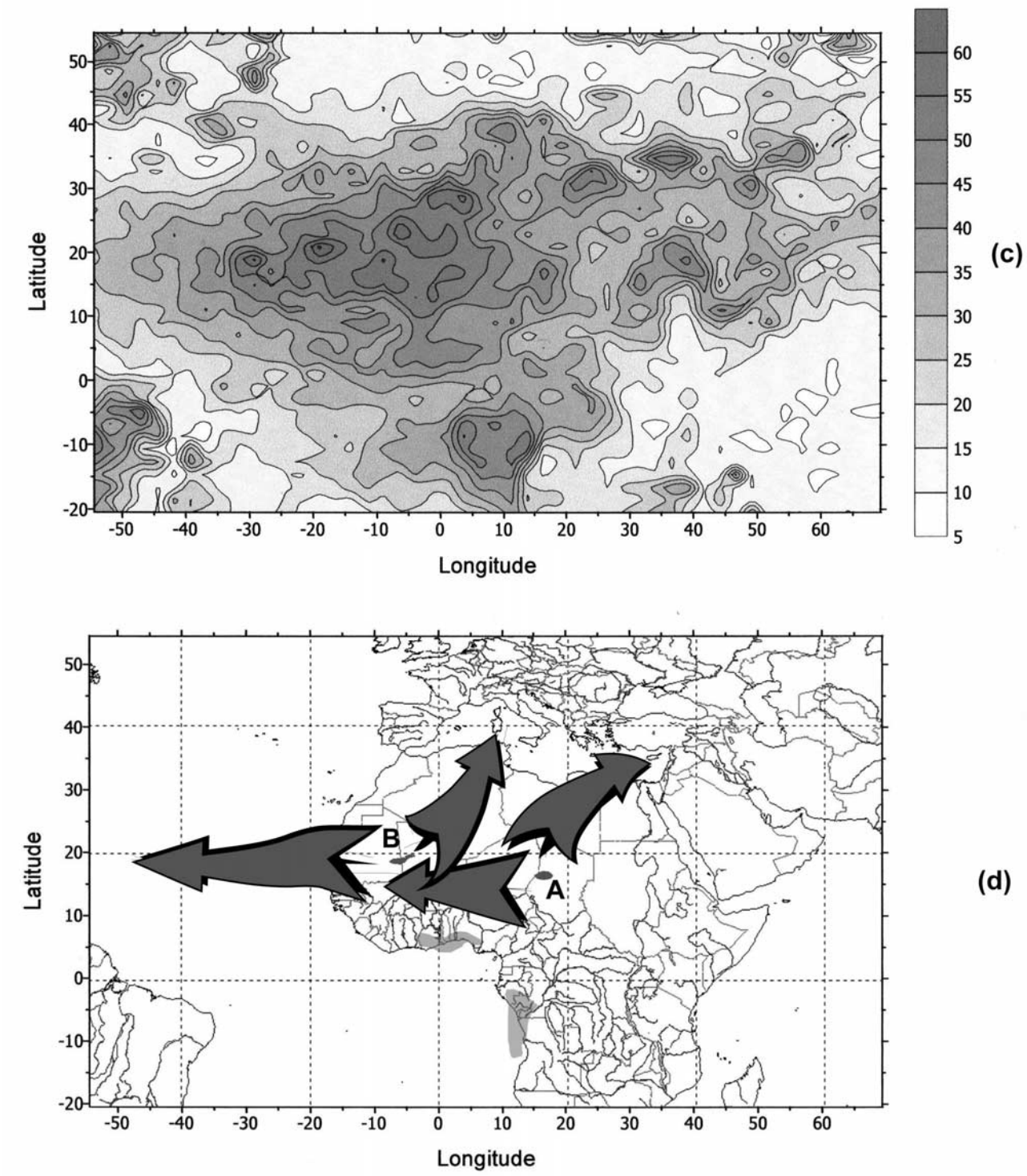

Figure 1. (continued)

[10] If we treat the aerosol index as a measure of the amount of aerosols, the local maxima of the AI distribution corresponds to the strongest sources of aerosols. Indeed, the continuity equation for the aerosol column density ρ is

$$\frac{\partial \rho}{\partial t} + \mathbf{v}\nabla\rho = A - S\rho$$

where A is the source term and S is the rate of loss. The average column density is

$$\langle\rho\rangle = \frac{A - \langle \mathbf{v}\nabla\rho\rangle}{S}$$

The local maxima of the average column density occur at the points where $\partial\langle\rho\rangle/\partial x = 0$, $\partial\langle\rho\rangle/\partial y = 0$. Hence, one can

expect that at these points $\langle \mathbf{v}\nabla\rho \rangle \approx 0$, and that the local maxima of the source term A approximately coincide with the local maxima of $\langle \rho \rangle$. Note, that we do not use threshold filters, but all positive values of aerosol index have been incorporated in the distributions under discussion.

[11] In fact, the aerosol index does not depend only on the column aerosol mass loading, but also on the other parameters of the aerosol. For our analysis, most important and most sensitive is the dependence of the AI on the height distribution of the aerosol index. We can neglect other dependencies, like the dependence on the scattering angles (since the orbit is Sun-synchronous), dependence on the size distribution etc., but the aerosol index dependence on the dust layer altitude is significant and, in principle, might affect our conclusions.

[12] Let the aerosol size and composition distribution be given. Then, the aerosol index increases monotonically with the increase of the amount of absorbing dust if the height distribution remains the same. However, the aerosol index also increases monotonically with the height of the aerosol layer if the amount of dust does not change. Therefore, the local maximum of the aerosol index in its instantaneous distribution may be associated either with the maximum of the aerosol amount, either with the maximum height of the aerosol layer, or with some combination of these parameters. Indeed, one can easily find many daily distributions with local aerosol maxima above, say, the sea surface. Therefore the local maxima positions indicate the main transport ways for the aerosols.

[13] However, in order to reveal dust sources, we average the aerosol distributions over long periods of time. Naturally, dust sources remain at the same places giving the largest input to the averaged AI value, whereas positions of local maxima along the transport paths vary from day to day and, after averaging,result in relatively uniform background.

[14] The presence of sub pixel clouds reduces randomly the value of the aerosol index as compared with its 'true' value, and resulting in slight reduction of the averaged value of the aerosol index. Hence the presence of sub pixel clouds does not affect our analysis, and it is reasonable to conclude that our analysis and determination of dust sources is correct.

[15] The following main sources of the UV-absorbing aerosols can be inferred from the Figure 1b: region *A* - centered at lat $\approx$ 16°N and long $\approx$ 16°E corresponding to the Chad basin and the wadi deltas leading out of mountainous areas of Ahaggar and Tibesti into the basin. The second major source region, region *B* - centered at lat $\approx$ 19°N and long $\approx$ 6°W corresponds to the Eljouf basin, again supplied with silt and clays through the wadis descending from the neighboring mountains. They are the primary sources of mineral dust for the Mediterranean basin. Two smaller local maxima can be seen in region *C* centered at lat. $\approx$ 33°N and long $\approx$ 7°E, and in region D at lat. $\approx$ 25°N and long $\approx$ 18°E. Aerosol sources in Northern Sudan and in the Arabian Peninsula can also be identified. Regions *E* (at lat. $\approx$ 5°N and long $\approx$ 2°E) and *F* (lat. $\approx$ 7°S and long $\approx$ 12°E) located near Central Africa's Atlantic coast, are associated with biomass burning. It is worth noting that the mineral dust sources *A–D* identified as local maxima of aerosol distribution coincide with the sources found by *Prospero et al.* [2002] as places of maximum frequency of occurrence of dust events. We refer the reader to [*Prospero et al.*, 2002] for detailed characterization of these sources.

[16] Figure 1c represents the distribution of the highest observed values of TOMS aerosol index for the period August, 1996 to April, 2000. Obviously, the largest values of AI occur along the main trajectories of the dust plumes. Figure 1d shows schematically the main directions of the aerosol transport.

[17] While region A seems to be a steady source of dust, region B shows periods with higher average values of AI (Figure 1c). This point is further illustrated by Figure 2a, which shows the dispersion of the aerosol index for the period of measurements:

$$\sigma = \left[\Sigma(AI - \langle AI \rangle)^2\right]^{1/2}$$

While regions *E* and *F* appear to be the most variable, they are clearly associated with biomass burning. Region *B*, on the other hand, reveals the strongest variability among all the sources of desert aerosols.

[18] The two main sources, A and B, as well as source C have the same surface properties as to propensity of dust formation. The difference in the variation with time of the two source regions, A and B + C, is probably to be found in the different meteorological conditions leading to dust formation. The atmosphere over source A, the Chad basin is under the influence of the steady Easterly winds at the southern edge of a system of high pressure. Perturbations in the flow in the form of Easterly Waves form semi- periodically in the Easterly flow South of the High and keep the dust supply from the Chad region in a more or less stationary regime from February to September with possibly a maximum in the spring after the drying out of the play a and its tributaries. The more Northern source C and the more Western source, B, may be activated by, in addition, travelling cyclone systems. These are instigated by wave intrusions invading over the Western Atlas ranges from the Atlantic, by European lows or by the Genoa low, invading over the more Eastern Atlas ranges. These travelling cyclone systems intensify on reaching the lee of the Atlas Mountains and can reach regions B and C mostly in spring and early summer, but also in the fall. They usually travel East and North afterwards.

[19] It is curious that the normalized distribution of the AI dispersion (i.e., $\sigma/\langle AI \rangle$) shown in Figure 2b exhibits rather clearly the coastlines of the region of interest (except for the Atlantic coast of Central Africa). One can easily identify in Figure 2 the North African coast along the Mediterranean, the Arabian Peninsula, Madagascar and even the Iberian peninsula and Asia Minor. However, there is no one to one relation between $\sigma/\langle AI \rangle$ above the sea and above the land surface. In the Northern African region (Sahara), $\sigma/\langle AI \rangle$ is larger above the sea than above the land, whereas in Europe or in Madagascar this relation is reversed. For this reason, it seems less probable that TOMS aerosol index is directly contaminated by the surface reflectivity. The most plausible explanation of coastlines' "visibility" in the distributions (Figures 1b, 1c, 2a, and, especially, 2b) is that the average wind direction is normal to the coastline (because of breeze). This is definitely not true for tropical West Africa,

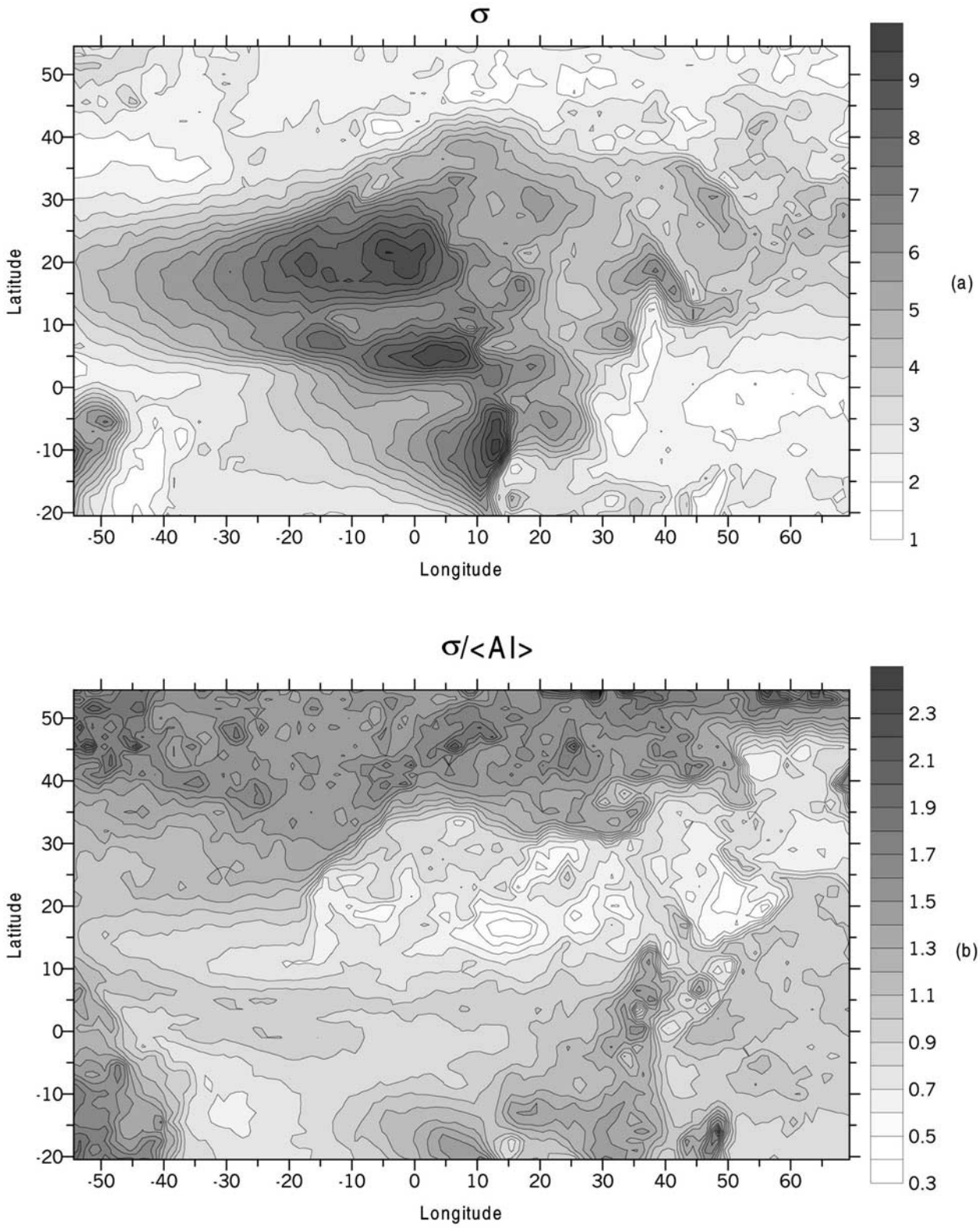

Figure 2. Distribution of dispersion (a) and normalized dispersion (b) of the aerosol index during the period of observation.

where the average wind direction is westward, and, indeed, the African Atlantic coast is not seen in the Figure 2b. Nonetheless, one cannot exclude the different behavior of aerosol sinks above the sea and the land surfaces. For example, the aerosol particles above a sea rapidly absorb moisture, grow in size, and, as a result, sediment faster [*Ganor and Foner*, 2001]. The lower "visibility" of the West African coast line may be due to the average optical

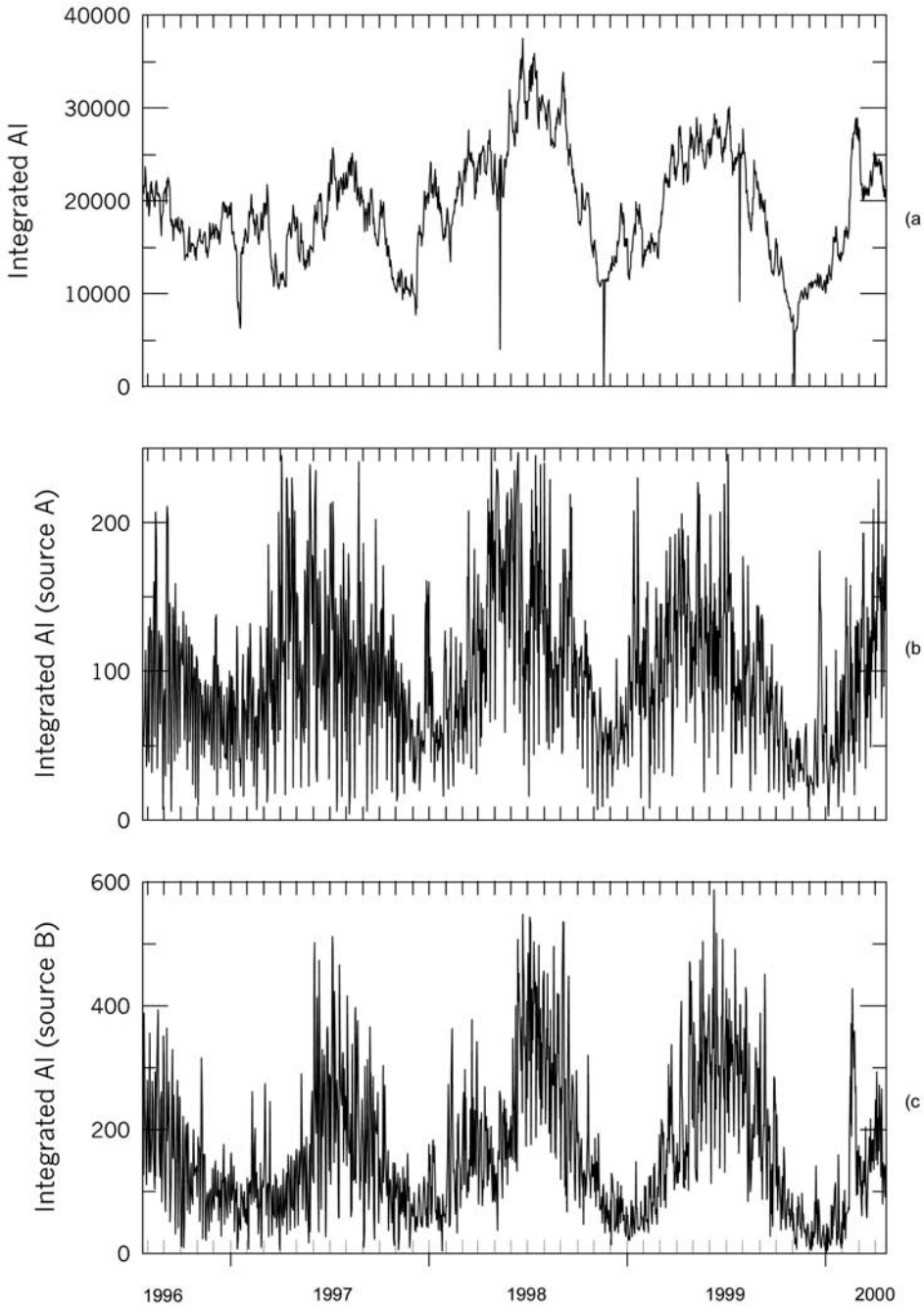

Figure 3. Daily values of the aerosol index integrated over the whole region of interest (a) and over small areas near the source regions A (b) and B (c).

depth there being larger and the decay of the latter slower with increasing distance from the shore.

[20] Figure 3a shows the daily values of the aerosol index integrated over the whole region of interest ($20.5°S \leq$ lat. $\leq 54.5°N$, $54°W \leq$ long $\leq 70°E$). This quantity, to a first approximation, can be used as a measure of the total amount of the Saharan desert aerosol in the atmosphere. The aerosol loading exhibits clear annual variations, it increases in spring-summer, and almost disappears in winter. The available amount of aerosol on each day is larger than its day-to-day variations due to different levels of dust storm activity. Daily values of the aerosol index integrated over small regions near the sources (Figure 3b: $16.5° \leq$ lat. $\leq 18.5°$, $18.125° \leq$ long $\leq 21.875°$ for region A; Figure 3c: $19.5° \leq$ lat. $\leq 22.5°$, $-14.375° \leq$ long $\leq -10.625°$ for region B) exhibit the same behavior: the annual variation of the average amount of the aerosol is comparable with the daily variations associated with dust storms.

[21] This means that during the spring the dust sources are more powerful than the sinks. It, therefore, implies that the desert aerosol particles are permanently available as a reservoir in the atmosphere above Northern Africa, even if there are no primary dust mobilization from the source regions A–D. Hence, the appearance of the desert dust in

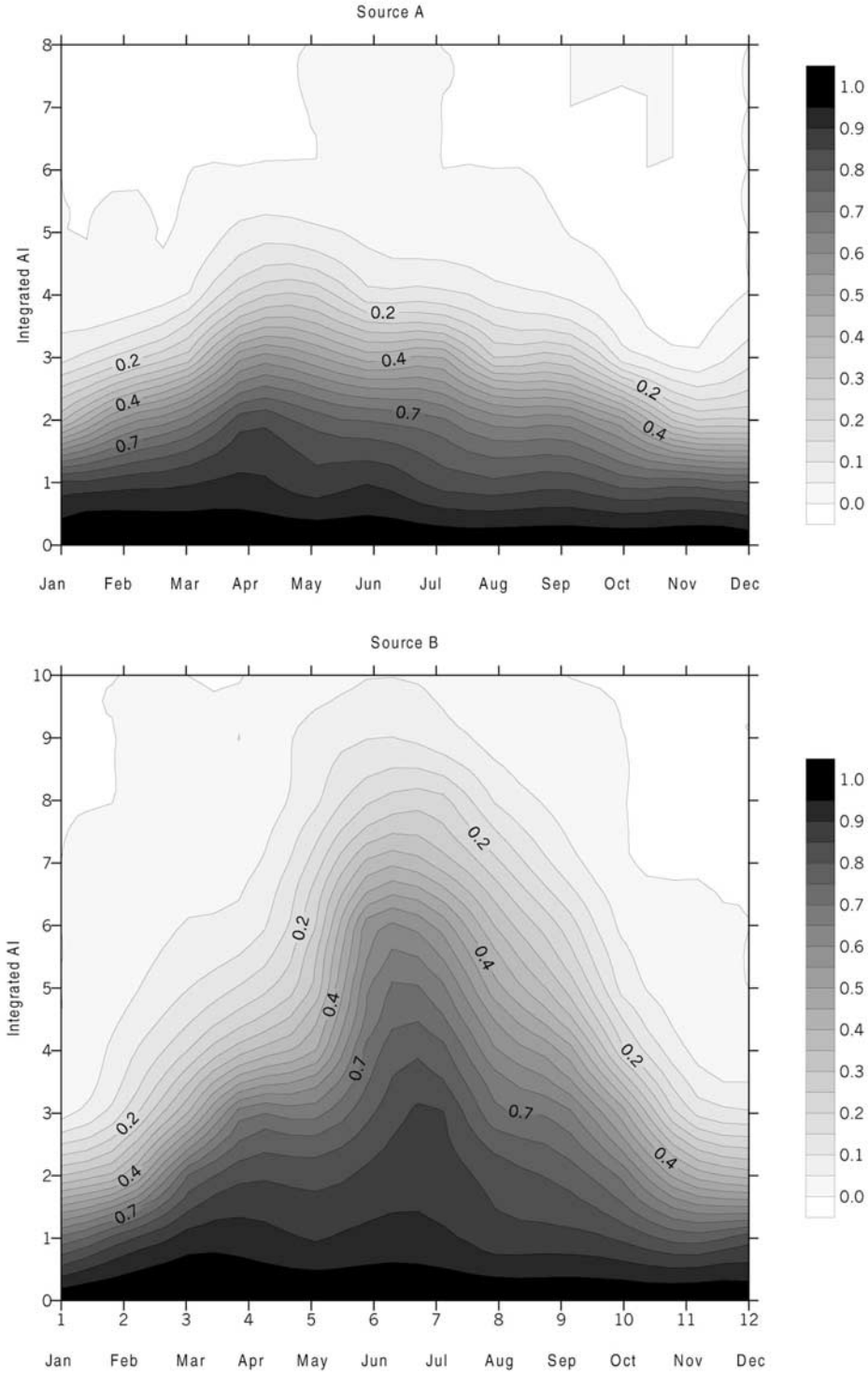

Figure 4. Distribution function for the dust occurrence probability near the source region A (a) and near the source region B (b).

the Mediterranean region is not necessarily always directly caused by the dust storms in the primary sources. It can be transported to the Mediterranean from the permanently existing reservoir of dust in the atmosphere above Northern Africa as soon as the appropriate synoptic conditions arise.

[22] We calculated the seasonal dependence of dust occurrence probability. Figure 4 represents 2D plots of the distribution function $F(t, AI_R)$ which is defined as the probability that at a given month t the daily aerosol index integrated over the region is larger than AI_R. The abscissa is the month of the year, and the ordinate corresponds to the integrated aerosol index. Shadow coding shows the value of the distribution function. The maximum dust loading is expected in spring (April) for the source region A

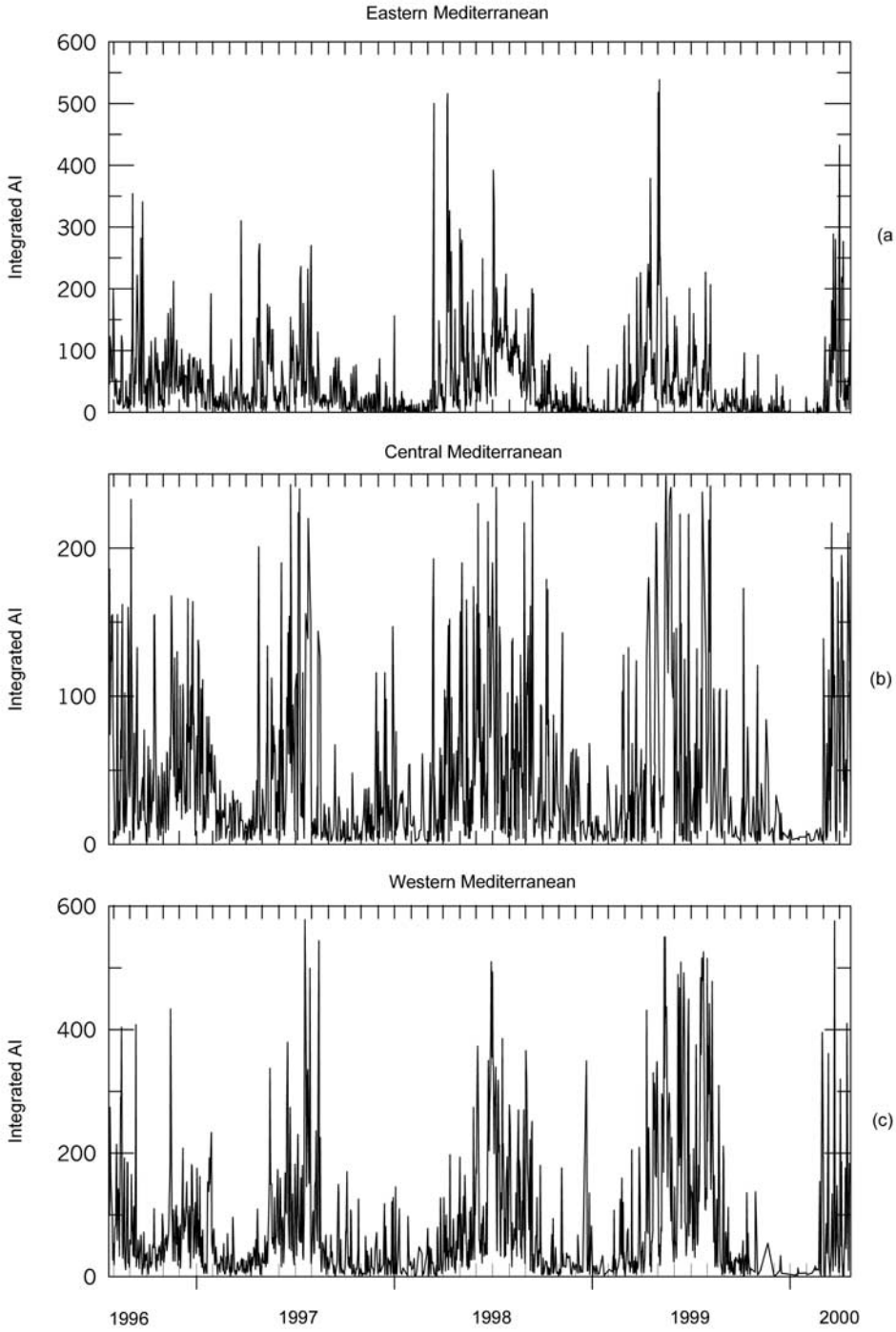

Figure 5. Daily values of the aerosol index integrated over the Eastern (a), Central (b), and Western Mediterranean (c).

(Figure 4a). Near the source region B, the maximum of the dust activity occurs in summer (July, Figure 4b).

4. Desert Dust Above the Mediterranean Region

[23] Figure 5 shows the daily values of the aerosol index integrated over the regions (a) in the Eastern ($35° \leq$ lat $\leq 40°$, $25 \leq$ long $\leq 35°$), (b) Central ($35° \leq$ lat $\leq 40°$, $12° \leq$ long $\leq 22°$), and (c) Western Mediterranean ($35° \leq$ lat $\leq 40°$, $0° \leq$ long $\leq 10°$). Contrary to the aerosol loading above the Sahara (Figure 3), there is no significant annual variation of the background amount of the aerosol present in the atmosphere. Instead, the annual variation is revealed in the amount of dusty days during different seasons and in the strength of the aerosol loading during these days. Between the dusty days, the loading remains low, as it can be seen from the Figure 6, showing the aerosol index integrated over the same regions with increased time resolution for May, 1998.

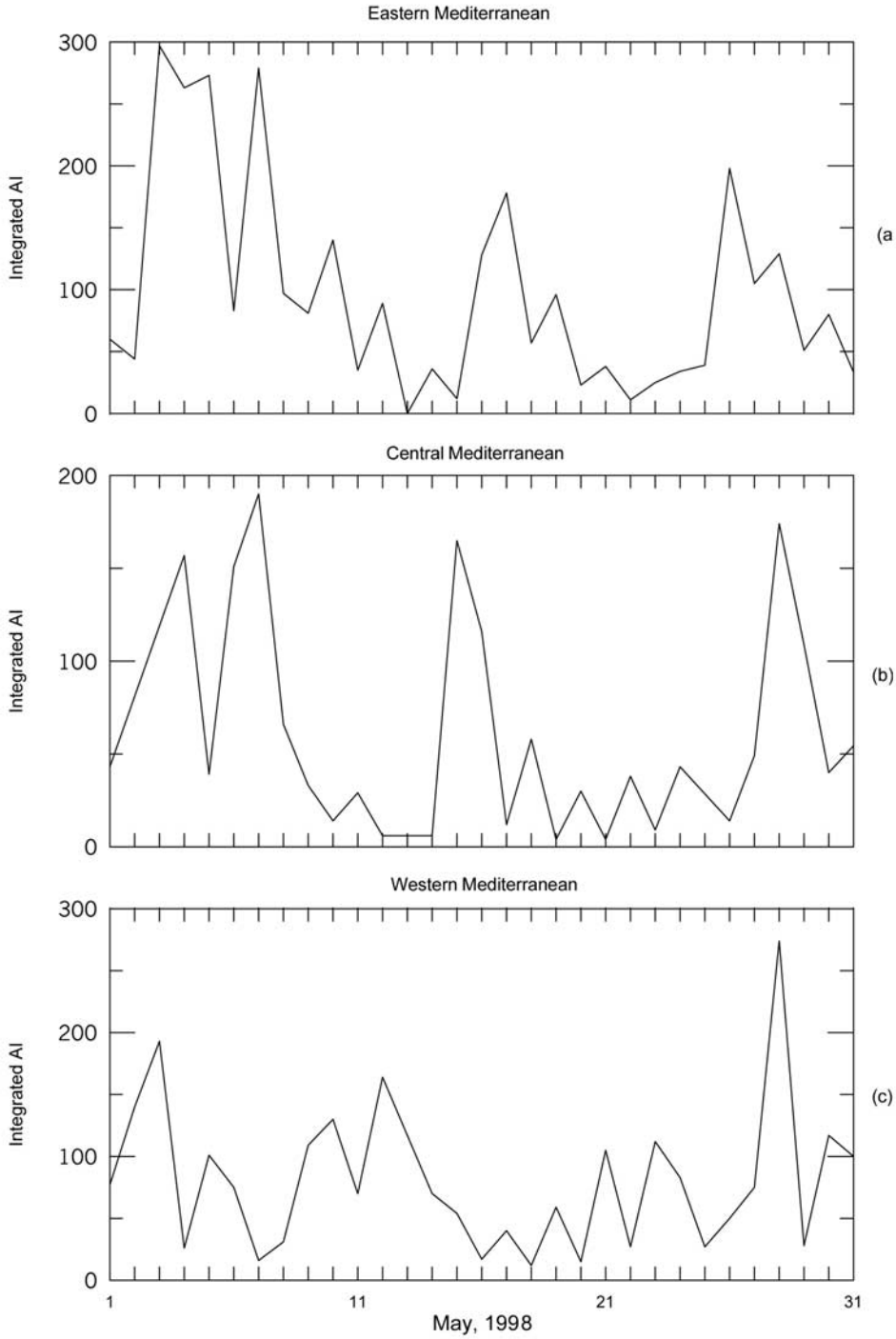

Figure 6. Daily values of the aerosol index integrated over the Eastern (a), Central (b), and Western Mediterranean (c) for May, 1998.

[24] Figure 7 represents the probability of dust occurrence for these regions in the same format as Figure 4. The maximum dust loading is expected in spring (April) for the eastern Mediterranean (Figure 7a), and in summer for the central Mediterranean (June, Figure 7b) and western Mediterranean (July, Figure 7c). These distributions are in good agreement with the *Moulin et al.* [1998] results.

[25] Seasonal occurrence of dust events for the eastern sector (Figure 7a) resembles that for the source region *A* (Figure 4a), whereas the distribution functions for central and western Mediterranean sectors are similar to that of source region *B* (Figure 4b). However, this does not mean that region A directly supplies the desert dust to the eastern Mediterranean, and region *B* is a direct primary source for the western and central sections.

[26] The clear difference between the distribution functions for the three sectors (Figure 7) can be explained by different dynamics of dust events in the Mediterranean

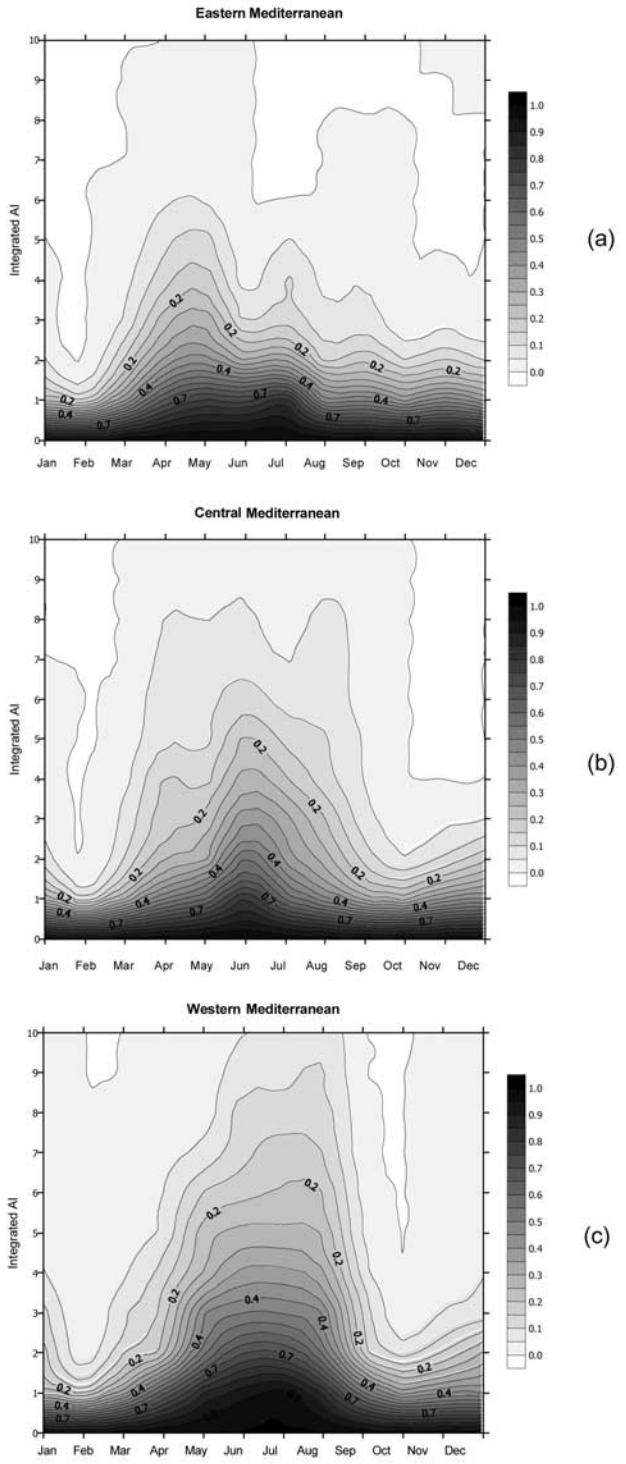

Figure 7. Distribution function for the dust occurrence probability in the Eastern (a), Central (b), and Western Mediterranean (c).

rather than by different sources. This is illustrated by the time variation of the aerosol index value above the Mediterranean taken along a certain latitude. Figure 8 shows the distribution of the aerosol index along the latitude 35.5° during the year 1999. The abscissa corresponds to the longitude, and the ordinate is the day of the year. The Mediterranean dust storm appears as a ''spot'' in such a

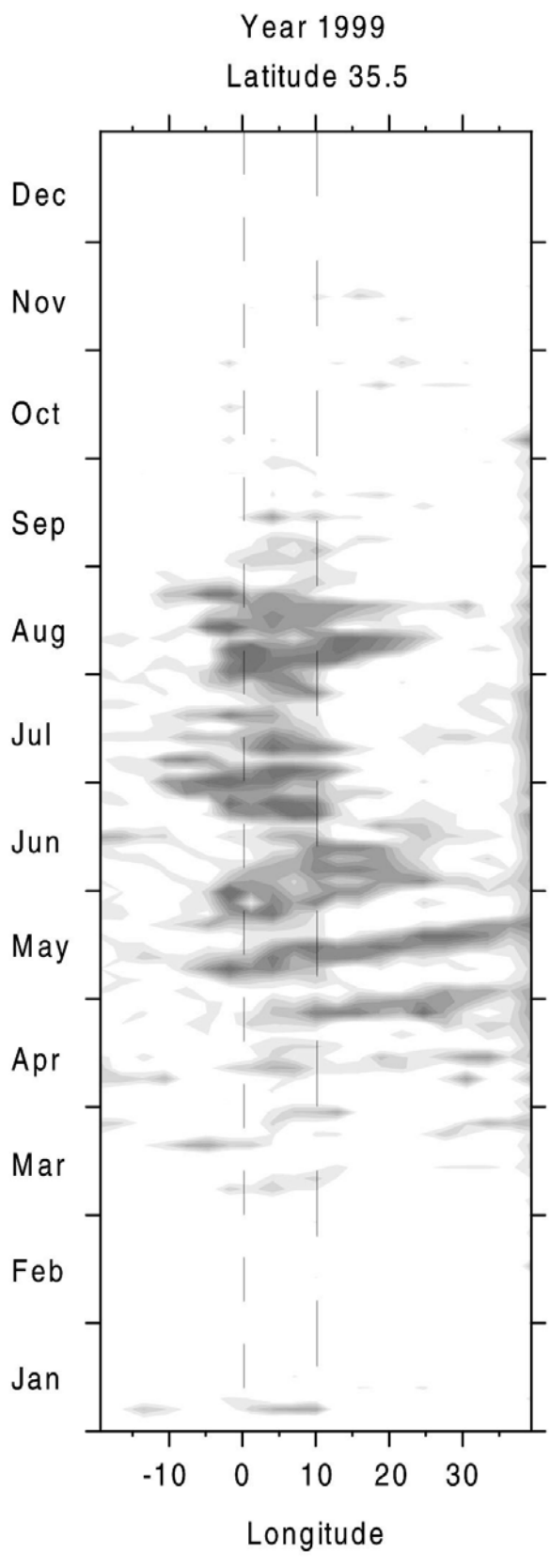

Figure 8. Daily distributions of the aerosol index in the Mediterranean along the latitude 35.5°.

presentation. One can see that there are no isolated dust storms in different sectors. Each dust storm occupies (during its life cycle) almost the whole length of the Mediterranean Sea. Almost each event starts in the western sector, and then propagates eastward. The eastward transport can be clearly seen as an inclination of the ''spot'' axis. This inclination remains almost the same for all the events, i.e., the eastward propagation occurs with the same velocity ($\sim$7–8 degrees/day) for all dust storms, independently of the season. In spring, the dust propagates without interruptions to the Eastern coast of the sea. In contrast, in summer the propagation of the dust is stopped at the longitude $\sim$10–15°. The reason for this could be the high pressure that develops over the central Mediterranean and blocks the eastward propagation of the dust, as was noted by *Moulin et al.* [1998], and/or southward deviation of the dust by the strong Etesian NW winds in the Eastern Mediterranean during summer, associated with the cyclonic circulation around the dominant heat low over the Middle-Eastern deserts. In autumn, the dust events penetrate the eastern sector again. This type of dynamics as well as the velocity of eastward displacement is typical for Sharav cyclones [*Alpert and Ziv*, 1998; *Alpert et al.*, 1990]. Thus, it is reasonable to assume that the dust events in the Mediterranean are not caused directly by the increased dust supply (dust storms) in the main source regions but by the occurrence of proper synoptic conditions. The role of the source region is to maintain the reservoir of desert aerosol above the whole of Northern Africa during spring-summer months (Figures 1b, 3a). The dust for Mediterranean region is mobilized and transported north- and eastwards from this reservoir each time a Sharav cyclone is formed.

[27] One more feature, which can be traced in Figure 8, is worthy of mentioning. The region between the longitudes 0°–10° (denoted by vertical dashed lines) is above the land surface. In this region, the aerosol index is slightly higher than in the adjacent areas above the surface, resulting in a vertical band of relatively enhanced intensity which can be seen in Figure 8. It is not clear, whether the aerosol loading is larger above the land as compared to the sea, or whether there is contamination of the reflecting surface BDRF in the aerosol index. This effect, however, does not mask the general dynamics of the dust events in the Mediterranean region inferred from the TOMS aerosol index.

5. Conclusion

[28] We proposed in this paper to identify local maxima of the averaged AI distribution with the sources of dust aerosol. Being simpler than the approach based on a dusty days occurrence [*Prospero et al.*, 2002], our method gives the same results. The TOMS aerosol index shows that during the period April–August, the whole region above the Northern Africa is almost permanently loaded with significant amounts of desert dust. The main, most powerful, sources of this dust are located in the regions centered at lat. $\approx$ 16° and long $\approx$ 16° and lat. $\approx$ 19° and long $\approx -6°$. During the spring-summer time the sinks do not compensate the dust supply by these sources. The Chad basin region at lat. $\approx$ 16° and long $\approx$ 16° is more stable, with maximum activity in April, and the region at lat. $\approx$ 19° and long $\approx -6°$ reveals a more variable dust supply with the maximum in July. The heat lows, called Sharav cyclones, form along the Mediterranean coastal zones of North Africa, primarily from March to June and travel West to East. These mobilize the available desert dust and transport it eastward and northward along the Mediterranean basin. A new method for description of dust plumes propagation (see Figure 8) was applied to the study of dust events in the Mediterranean Sea and enabled us to follow their dynamics. Identifiable dust plumes appear first in the Western sector of the sea, and then moves eastward with the speed of 7–8 degrees/day, corresponding to the average motion of the Sharav cyclone. In spring, this motion continues at least up to the eastern coast of the sea. In summer, the dust plume does not penetrate longitudes to the east of $\sim$15°.

[29] **Acknowledgments.** This work was supported by the Israeli Ministry of Science, Culture and Sports in the framework of the MEIDEX project. We appreciate discussions with Omar Torres and Paul Ginoux.

References

Alpert, P., and E. Ganor, A jet stream associated heavy dust storm in the western Mediterranean, *J. Geophys. Res.*, *98*, 7339–7349, 1993.

Alpert, P., and E. Ganor, Sahara mineral dust measurements from TOMS - Comparison to surface observations over the Middle East for the extreme dust storm, 14–17 March 1998, *J. Geophys. Res.*, *106*, 18,275–18,286, 2001.

Alpert, P., and B. Ziv, The Sharav Cyclone - Observation and some Theoretical Considerations, *J. Geophys. Res.*, *94*, 18,495–18,514, 1989.

Alpert, P., B. U. Neeman, and Y. Shay-el, Climatological analysis of Mediterranean cyclones using ECMWF data, *Tellus, Ser. A*, *42*, 65, 1990.

Alpert, P., Y. J. Kaufman, Y. Shay-El, D. Tanre, A. da Silva, and J. H. Joseph, Quantification of dust-forced heating of the lower troposphere, *Nature*, *395*, 367–370, 1998.

Bergametti, G., A.-L. Dutot, P. Buat-Menard, R. Losno, and E. Remoudaki, Seasonal variability of the elemental composition of atmospheric aerosol over the northwestern Mediterranean, *Tellus, Ser. B*, *41*, 353, 1989.

Dayan, U., J. L. Heffter, J. M. Miller, and G. Gutman, Dust intrusion events into the Mediterranean basin, *J. Appl. Meteorol.*, *30*, 1185–1199, 1991.

Ganor, E., The frequency of Saharan dust episodes over Tel Aviv, Israel, *Atmos. Environ.*, *28*, 2867–2871, 1994.

Ganor, E., and H. A. Foner, The Mineralogical and chemical properties and the behavior of Aeolian Saharan Dust over Israel, in *The Impact of Desert Dust Across the Mediterranean*, edited by S. Guerzoni and R. Chester, pp. 163, Kluwer Acad., Norwell, Mass., 1996.

Ganor, E., and H. A. Foner, Mineral dust concentrations, deposition fluxes and deposition velocities in dust episodes over Israel, *J. Geophys. Res.*, *106*, 18,431–18,438, 2001.

Herman, J. R., P. K. Bhartia, O. Torres, C. Hsu, C. Seftor, and E. Celarier, Global distributions of UV-absorbing aerosols from Nimbus 7/TOMS data, *J. Geophys. Res.*, *102*, 16,911–16,922, 1997.

Hsu, N. C., J. R. Herman, O. Torres, B. N. Holben, D. Tanre, T. F. Eck, A. Smirnov, B. Chatenet, and F. Lavenu, Comparisons of the TOMS aerosol index with Sunphotometer aerosol optical thickness: Results and applications, *J. Geophys. Res.*, *104*, 6269–6280, 1999.

Joseph, J. H., The sensitivity of a numerical model of the global atmosphere to the presence of a desert aerosol, in *Aerosols and their climatic effects*, pp. 215–226, A. Deepak, Hampton, Va., 1984.

Joseph, J. H., and N. Wolfson, The ratio of absorption to back-scatter of solar radiation during Khamsin conditions and effects on the radiation balance, *J. Appl. Meteorol.*, *14*, 1389–1396, 1975.

Joseph, J. H., A. Manes, and D. Ashbel, Desert aerosols transported by Khamsinic depressions and their climatic effects, *J. Appl.*, *12*, 792–797, 1973.

Karyampudi, V. M., et al., Validation of the Saharan dust plume conceptual model using lidar, Meteosat and ECMWF, *Bull. Am. Meteorol. Soc.*, *80*, 1045–1075, 1999.

Kaufman, Y. J., D. Tanre, H. R. Gordon, T. Nakajima, J. Lenoble, R. Frouin, H. Grassl, B. M. Herman, M. D. King, and P. M. Teillet, Passive remote sensing of tropospheric aerosol and atmospheric correction for the aerosol effect, *J. Geophys. Res.*, *102*, 16,815–16,830, 1997.

Kaufman, Y. J., et al., Smoke, clouds, and radiation Brazil (SCAR-B) experiment, *J. Geophys. Res.*, *103*, 31,783–31,808, 1998.

Kubilay, N., and A. C. Saydam, Trace elements in atmospheric particulates

over the eastern Mediterranean: Concentrations, sources, and temporal variability, *Atmos. Environ.*, *29*, 2289–2300, 1995.

Levin, Z., and J. D. Lindberg, Size distribution, chemical composition and optical properties of urban and desert aerosols in Israel, *J. Geophys. Res.*, *84*, 6941–6950, 1979.

Levin, Z., J. H. Joseph, and Y. Mekler, Properties of Sharav (Khamsin) dust - comparison of optical and direct sampling data, *J. Atmos. Sci.*, *37*, 882–891, 1980.

Levin, Z., E. Ganor, and V. Gladstein, The effects of desert particles coated with sulfate on rain formation in the eastern Mediterranean, *J. Appl. Meteorol.*, *35*, 1511–1523, 1996.

Loye-Pilot, M. D., and J. M. Martin, Saharan dust input to the western Mediterranean: An eleven years record in Corsica, in *The Impact of Desert Dust Across the Mediterranean*, edited by S. Guerzoni and R. Chester, pp. 191–200, Kluwer Acad., Norwell, Mass., 1996.

Manes, A., and J. H. Joseph, Secular and seasonal variations of the atmospheric turbidity in Israel at Jerusalem, *J. Appl. Meteorol.*, *10*, 487–492, 1971.

Marticorena, B., and G. Bergametti, Two-year simulations of seasonal and interannual changes of the Saharan dust emissions, *Geophys. Res. Lett.*, *23*(15), 1921–1924, 1996.

Molinaroli, E., S. Guerzoni, and G. Rampazzo, Contribution of the Saharan dust to the central Mediterranean basin, *Geol Soc. Am.*, *284*, 303–312, 1993.

Moulin, C., F. Guillard, F. Dulac, and C. E. Lambert, Long-term daily monitoring of Saharan dust load over ocean using Meteosat ISCCP-B2 data, 1, Methodology and preliminary results for 1983–1994 in the Mediterranean, *J. Geophys. Res.*, *102*, 16,947–16,958, 1997.

Moulin, C., et al., Satellite climatology of African dust transport in Mediterranean atmosphere, *J. Geophys. Res.*, *103*, 13,137–13,144, 1998.

Prospero, J. M., P. Ginoux, O. Torres, S. E. Nicholson, and T. E. Gill, Environmental characterization of global sources of atmospheric soil dust identified with the NIMBUS 7 Total Ozone Mapping Spectrometer (TOMS) absorbing aerosol product, *Rev. Geophys.*, *40*(1), 1002, doi:10.1029/2000RG000095, 2002.

Sokolik, I. N., and O. B. Toon, Incorporation of mineralogical composition in two models of the radiative properties of mineral aerosol from Uv to IR wavelengths, *J. Geophys. Res.*, *104*, 9423–9444, 1999.

Tegen, L., A. A. Lacis, and I. Fung, Contribution of mineral aerosols from disturbed soils on the global radiation budget, *Nature*, *380*, 419–422, 1996.

Torres, O., P. K. Bhartia, J. R. Herman, and Z. Ahmad, Derivation of aerosol properties from satellite measurements of backscattered ultraviolet radiation: Theoretical Basis, *J. Geophys. Res.*, *103*, 17,099–17,110, 1998.

Torres, O., P. K. Bhartia, J. R. Herman, A. Sinyuk, P. Gionoux, and B. Holben, A long term record of aerosol optical thickness from TOMS observations and comparison to AERONET measurements, *J. Atmos. Sci.*, *59*, 398–413, 2002.

E. Ganor, P. L. Israelevich, J. H. Joseph, and Z. Levin, Department of Geophysics and Planetary Sciences, The Raymond and Beverly Sackler Faculty of Exact Sciences, Tel Aviv University, Ramat Aviv 69978, Israel. (peter@jupiter1.tau.ac.il)